*Geophys. J. Int.* (2002) **149,** 589–598

# Some dynamical characteristics of microseism time-series

Antoni M. Correig and Mercè Urquizú

*Departament d'Astronomia i Meteorologia, UB and Laboratori d'Estudis Geofísics "Eduard Fontserè," IEC Marti Franques* 1, E-08028 *Barcelona, Spain. E-mail: Ton.Correig@am.ub.es*

Accepted 2001 September 25. Received 2001 September 20; in original form 2000 September 12

## SUMMARY

Microseism time-series are non-stationary, non-linear and stochastic, and these characteristics can be reproduced by a forced non-linear damped oscillator. In the present study we show that such an oscillator is also able to explain other widely observed features, such as the variation, for a given seismic station, of the frequency of the secondary peak; the variation of the frequency of the primary peak for different seismic stations relative to the same source; the variations of amplitude of the power spectrum for stormy days with respect to quiet days; and the incoherent propagation of microseisms. Numerical simulations with the proposed phenomenological model suggest i) that the main spectral peak may be due to a competitive process between the resonant response of the medium and an external harmonic force (Longuet–Higgins model), ii) that the secondary peak may be generated by the process associated with the activity of the coastal waves or as a subharmonic of the resonant frequency and iii) that the large amplitude variations between quiet and stormy days refers in fact to variations in the source (storm) distance. From a general point of view we can say microseism activity can be interpreted as the resonant response of the Earth to atmospheric cyclonic storms coupled with the oceans.

**Key words:** numerical techniques, seismic noise, seismic spectra.

## 1 INTRODUCTION

Microseisms are worldwide phenomena usually understood as strong background noise, temporally and spatially varying, which strongly influences the detection of transient wave arrivals. As described by Aki & Richards (1980), two maxima of the power spectrum, at about 0.07 Hz, the primary peak, and 0.14 Hz, the secondary peak, are typical features of almost all the recordings at seismic stations. The primary peak is usually less intense than that the secondary one and, as proposed first by Wiechert in 1904, has been attributed to the direct impact of ocean waves on nearby coasts, since it roughly coincides with the primary peak of ocean wave oscillations. The most intensive peak was interpreted by Longuet-Higgins (1950) as the result of fluctuations of pressure caused by standing waves along the seabed.

The existence of the two above-mentioned peaks (although the primary peak may be absent) can be considered as a basic feature of seismic noise, which may suffer some shift in the frequency location of the two peaks from place to place (although preserving an approximate relation 2:1) and strong amplitude variations, (up to two orders of magnitude), due either to the location of the seismic station in quiet or noise places or, if in the same place, to the presence or absence of storm waves at sea. The above observations can be summarized by saying that the shape of the power spectrum is preserved.

In his review on microseism studies, Bath (1973) states that 'the studies of microseisms, the steady unrest of the ground, is a borderline field between meteorology, oceanography and seismology. Microseisms are no doubt of greatest concern to seismologists, but when their generation is to be explained, recourse must be taken to meteorological and oceanographic conditions. As a consequence, microseisms constitute a random process, like atmospheric turbulence and ocean surface waves.' No further comments appear in Bath's book on the characteristics of microseism time-series and, as far as we know, microseisms have only been analysed from the point of view of spectral (i.e. linear) analysis. At the same time, it is commonly accepted now (see Webb 1998; Kibblewhite & Wu 1991, and the references therein) that the principal mechanism for the generation of microseism oscillations (i.e. the source mechanism) is intrinsically non-linear: two ocean waves travelling in opposite directions, if certain resonant conditions for their frequencies are met, can give rise to an elastic (or seismoacoustic) wave that spreads up to thousands of kilometres from its source location under the seabed and is eventually recorded as a microseism.

In this study an attempt is made to look at the microseism phenomenon from a different viewpoint than that of seismic detection, by considering the 3-phase system atmosphere, hydrosphere (ocean or lake) and solid earth as a coupled non-linear dynamical system that generates microseism oscillations as a result of its complex dynamics. Accordingly, we consider the microseism time-series as a

signal that brings information relative to this complex dynamical system. Such an approach is close in spirit (e.g. from the point of view of the time-series analysis) to the study of fully developed turbulent flow in hydrodynamics, when a scalar time-series, say, of fluid velocity is measured at some point to extract qualitative information on the extended multidimensional system. To gain a deeper insight into the dynamics of microseisms, microseism time-series were analysed from the point of view of dynamical systems by Correig & Urquizu (1999) (hereafter referred to as CU), in an attempt to determine whether they are linear or non-linear, deterministic or stochastic. It should be noted at this point that in analysing observed noisy time-series, the results are often ambiguous, usually due to the fact that the time-series do not satisfy the hypothesis on which the method is based. For example, many methods have been designed under the hypothesis that the time-series is stationary (as for example the computation of the correlation dimension), which in our case is not satisfied. To overcome these difficulties, Theiler & Prichard (1996) and Schreiber (1998) propose the comparison of observations with computer generated time-series with well controlled statistical properties. We have followed this procedure, and as a first approximation to the mathematical description of microseisms, the model of a non-linear damped oscillator with multifrequency external excitation has turned out to be useful. Another question in analysing non-linear time-series is which are the invariants of the underlying dynamical system; that is, which parameters remain constant as the system evolves. For a linear system the invariant is the time-series itself, and any model has to be able to predict it through a (reduced) number of parameters. However, in dealing with chaotic or stochastic systems the time-series is no longer an invariant due to the sensitivity to the initial conditions or to the intrinsic randomness. In chaotic systems the invariants are the correlation dimension, Lyapunov exponents and Kolmogorov entropy. In the present study, however, no invariants have been found. Thus, our goal has been to look for a mathematical model able to reproduce the main characteristics of the observed time-series, that is their statistical properties in a generalized sense (non-stationarity, autocorrelation, coherence time, redundancy, etc., see Appendix), and the properties of the motion in phase space. The real invariants in dynamical systems are the statistical properties of the time-series and the motion in phase space.

Hasselmann (1963) performed a study of the origin of microseisms from a statistical analysis point of view and explicitly formulated the displacement field in terms of resonances of a layered elastic motion, a basic phenomenon in our interpretation. Hasselmann centred his study on the spectrum of the primary and secondary peaks, the so-called teleseismic microseisms, covering a frequency interval from about 0.05 Hz to about 1 Hz through the computation of the transfer function of a layered medium due to the action of a random distribution of external forces. The aim of the present study is to present a phenomenological model able to explain the seismic microseism spectrum for a wider interval, from about 0.01 Hz to 10 Hz, the interval well covered by broad-band seismic stations, that include the infra-gravity waves as well as the high frequency local noise. Contrary to Hasselmann, the model we actually propose is not derived from first principles, but rather designed to capture the main statistical characteristics of observations, which has proved to be a powerful tool in numerical simulations. In some sense, our model can be viewed as a generalization of Hasselmann's, including non-linearity and noise as an external force.

## 2 MAIN FEATURES OF MICROSEISM TIME-SERIES

Fig. 1 displays a short interval of two microseism time-series (vertical component) recorded at the broad-band seismic station CAD in the eastern Pyrenees, at about 50 km from the sea (Vila 1998) for a quiet day (b) and for a stormy day (a). Fig. 2 displays their corresponding power spectra; the location of the two main peaks are at 0.07 Hz and 0.2 Hz. Figs 1 and 2 are striking. Apart from the scaling, they display the same spectral characteristics for a stormy day as for a quiet day. Fig. 1 shows that, apart from the differences in the scale of amplitudes and the time-series of the quiet day being poorer in low frequencies, both seismograms display the same kind of modulations, roughly defining two wave packets of length $\sim$17 s and $\sim$70 s, each composed of oscillations of $\sim$5 s period. From Fig. 2 we can see that the 5 s period oscillation corresponds to the main peak of $\sim$0.2 Hz, the wave packet of 17 s to the primary peak located at $\sim$0.07 Hz, and the wave packet of 70 s to a very low-frequency peak located at $\sim$0.016 Hz. Following Webb (1998), the peaks located at 0.2 Hz and 0.07 Hz correspond to teleseismic microseisms, whereas the 0.016 Hz peak corresponds to infra-gravity waves. The two teleseismic microseism peaks of the spectra appear to be too wide to be considered as spectral lines corresponding to Fourier components. Although we cannot exclude *a priori* that both peaks correspond to the superposition of several incommensurate frequencies (Abarbanel *et al.* 1993), the broadness of these peaks suggest we could be in the presence of chaotic or stochastic processes. Accordingly, a rigourous time-series analysis has been performed.

In the previously mentioned study, CU analysed 50 seismic records of microseism time-series, all recorded at CAD station (Vila 1998), in a 30 min time window interval, starting at 03:00 and with a sampling rate of 80 Hz. The methodology was that of dynamical systems (Abardanel 1993; Kantz & Schreiber 1997). As the former paper is in Spanish, a brief account is provided in the Appendix. The main results are the following:

(1) Microseism time-series are non-stationary.
(2) Microseism time-series are stochastic.
(3) From the point of view of data analysis, there is strong evidence in favour of a non-linear character of microseism time-series.

The same results (i.e. non-stationarity, stochasticity and non-linearity) were also obtained for time-series generated by a Duffing oscillator (Guckenheimer & Holmes 1997), as well as for a $n$-well potential forced oscillator, having added, in both cases, additive noise to account for stochasticity. It is worth pointing out that the results were the same for both observations and generated time-series for all applied tests (see CU). Hence, we have adopted a Duffing oscillator with noise as a toy model for the study of microseism time-series.

Further, inland observations, widely reported, provide us with the following constraints:

(4) For a given seismic station, the central frequency of the main spectral peak may suffer slight variations, following the time variations of the source of cyclonic storms.

(5) For a cyclonic storm fixed in space, the central frequency of the main spectral peak may be shifted when comparing different seismic stations.

(6) By comparing records corresponding to stormy and quiet days (see Fig. 2), the location of the spectral peaks is preserved, and for frequencies higher than 2 Hz the corresponding power spectra tend to coalesce to the same level.

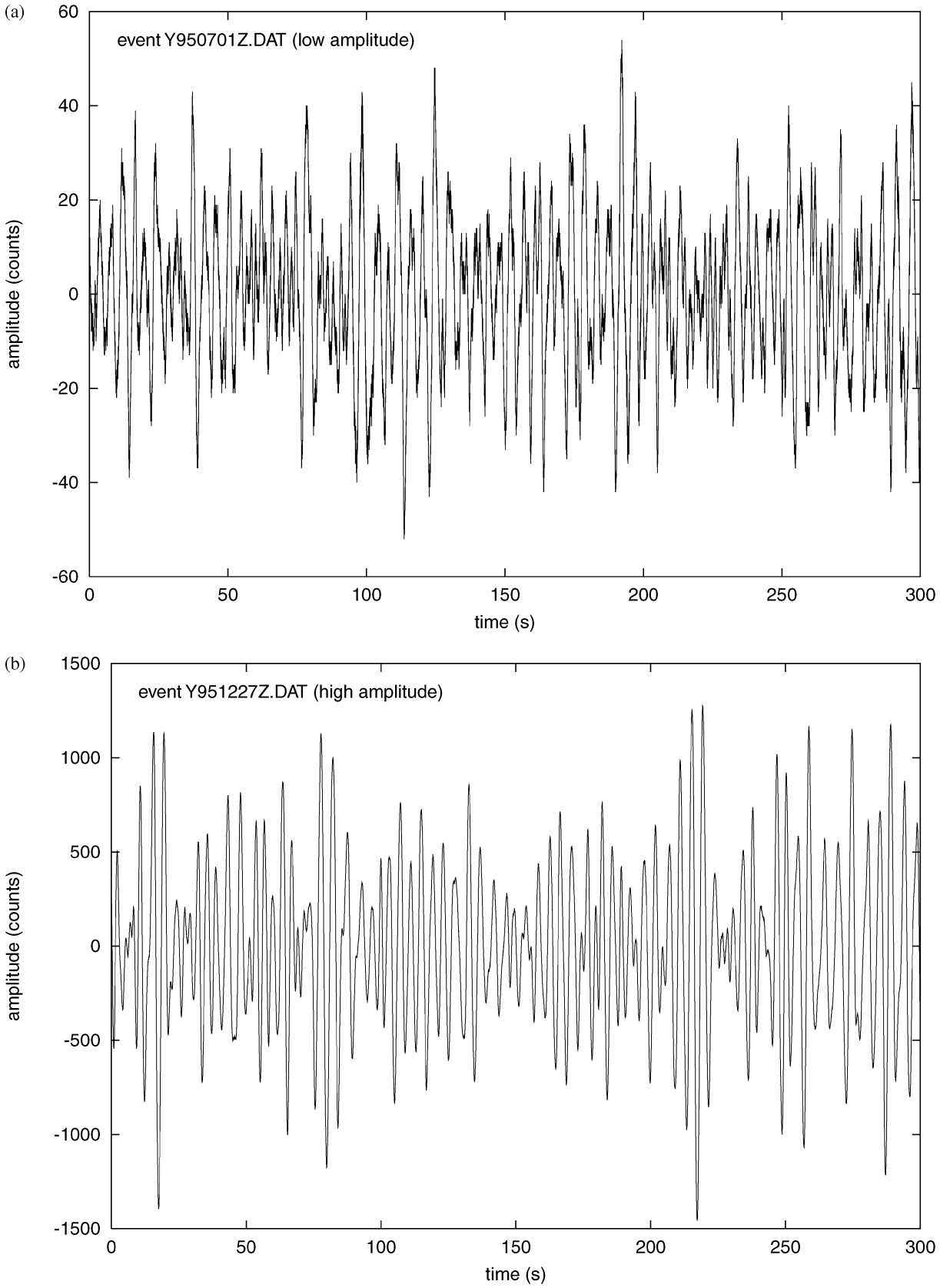


**Figure 1.** Examples of microseisms of large amplitude (951227) recorded during a cyclonic storm (a) and of low amplitude (950701) recorded during a quiet day (b). Note the difference in amplitude scales. All seismograms (velocity records) are measured in *counts*. 1 *count* = 0.345 $\mu s^{-1}$ = 3.45 × $10^{-8}$ m $s^{-1}$.

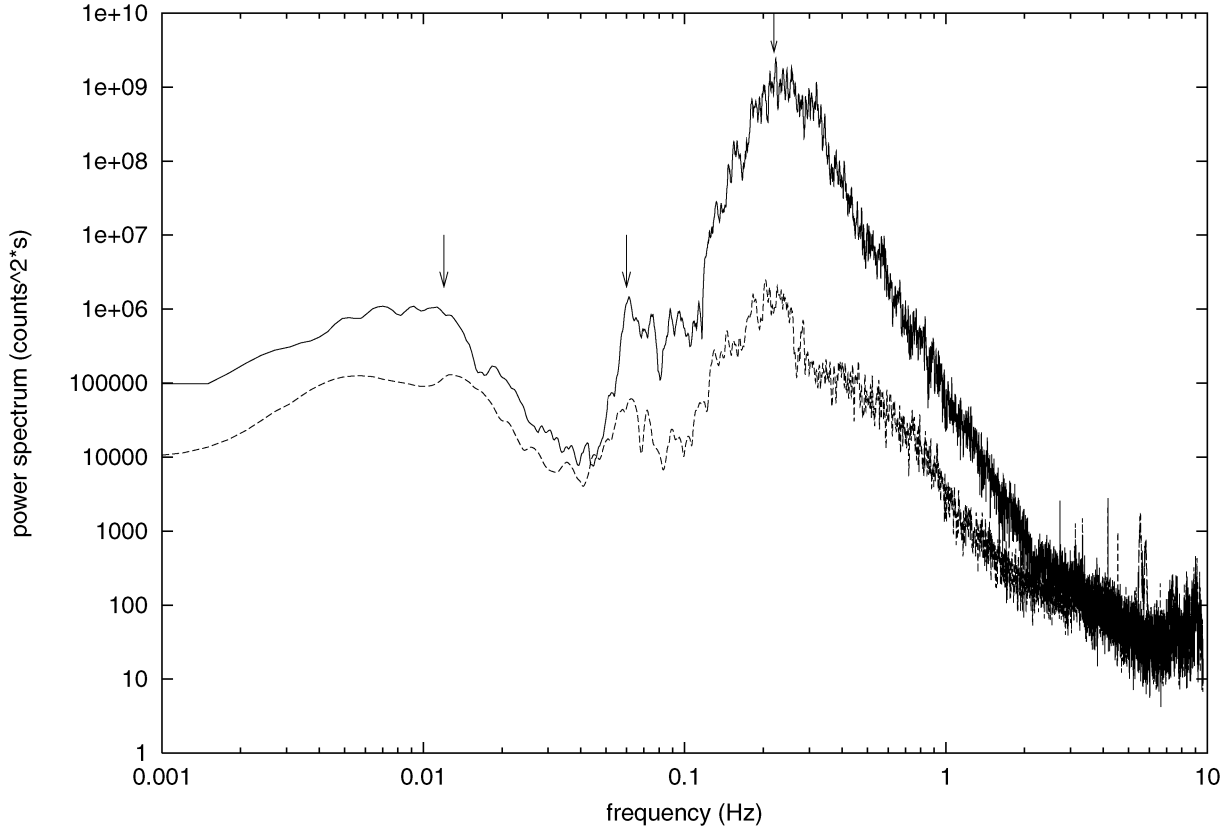


**Figure 2.** Power spectra of the high and low amplitude microseisms of Fig. 1.

(7) Microseisms propagate incoherently.

Observation (4) can be interpreted in terms of time variations of the external harmonic force and observation (5) as medium lateral variations. Observation (6) can be interpreted in the following way: the high frequency contents of microseisms can be attributed to local weather conditions as well as cultural noise (traffic, industrial activities, etc.), and it has been observed that the high frequency contents are clearly stochastic and as such has been modelled in studies of local seismic medium response (Lachet & Bard 1994; Morikawa *et al.* 1998). From now on, we will consider the high frequency stochastic interval as noise, whereas the remaining low frequency interval, where microseism and infra-gravity waves are located, as signal. It is also well known that microseisms propagate incoherently, so that their corresponding phase can be considered as random (as confirmed through the generation of surrogate data), thus accounting for observation (7). At this point it is worth pointing out that the following study has to be considered as a mean field one, in the sense that it is our purpose to explain average properties that may suffer important fluctuations. Compare, for example, Fig. 2, a typical display, with Fig. 3 (also a record from CAD station), in which the main peak has been split into two and shifted to lower frequencies, (0.115 Hz and 0.180 Hz instead of that of 0.2 Hz of Fig. 2), and in which the primary peak is not present. This figure constitutes a good example of the large fluctuations that the standard picture suffers.

## 3 MODEL DESCRIPTION

As previously stated, CU found that a Duffing oscillator with additive noise was able to generate time-series that capture the main characteristics (observations 1–3) of microseisms, as well as by using oscillators with more general potentials, suggesting that any non-linear forced oscillator with additive noise could be used to simulate the observed microseism time-series. Hence, as a starting point we will centre our interest in the classical and well studied Duffing oscillator:

$$\ddot{q} + \delta\dot{q} - \alpha q + \beta q^3 = \gamma\cos(\omega t) \tag{1}$$

where $\delta$ is the coefficient of damping, $\alpha$ the proper or resonant frequency of the system in the absence of external forces, $\beta$ the coefficient of non-linearity and $\gamma$ the amplitude of the external harmonic force. In the following we will generalize our model eq. (1) to be able to account for the observational constraints described in the preceding section. As it is well known, a Duffing oscillator generates time-series that may be periodic, quasi-periodic or chaotic, but not stochastic, hence the need to add white noise to the external force. This white noise can account for observation [6] in the sense that local high frequency noise contents may act as a driving force. It was also found that to generate a time-series qualitatively similar to the observed one, we had to add a second harmonic force with a driving frequency of about 0.015 Hz (corresponding to the 70 s period wave packet, the infra-gravity wave), added to an harmonic force with driving frequency of 0.2 Hz (the secondary microseism peak) as observed in the recorded microseisms; there is no need to add a third harmonic force to account for the primary peak at half the frequency of the secondary one because it appears naturally as a subharmonic. Whereas the last frequency is related to the oceanic standing wave, the infra-gravity wave with a predominant frequency of 0.015 Hz could be related to wind waves (Wells 1986). Eq. (1) is thus rewritten as:

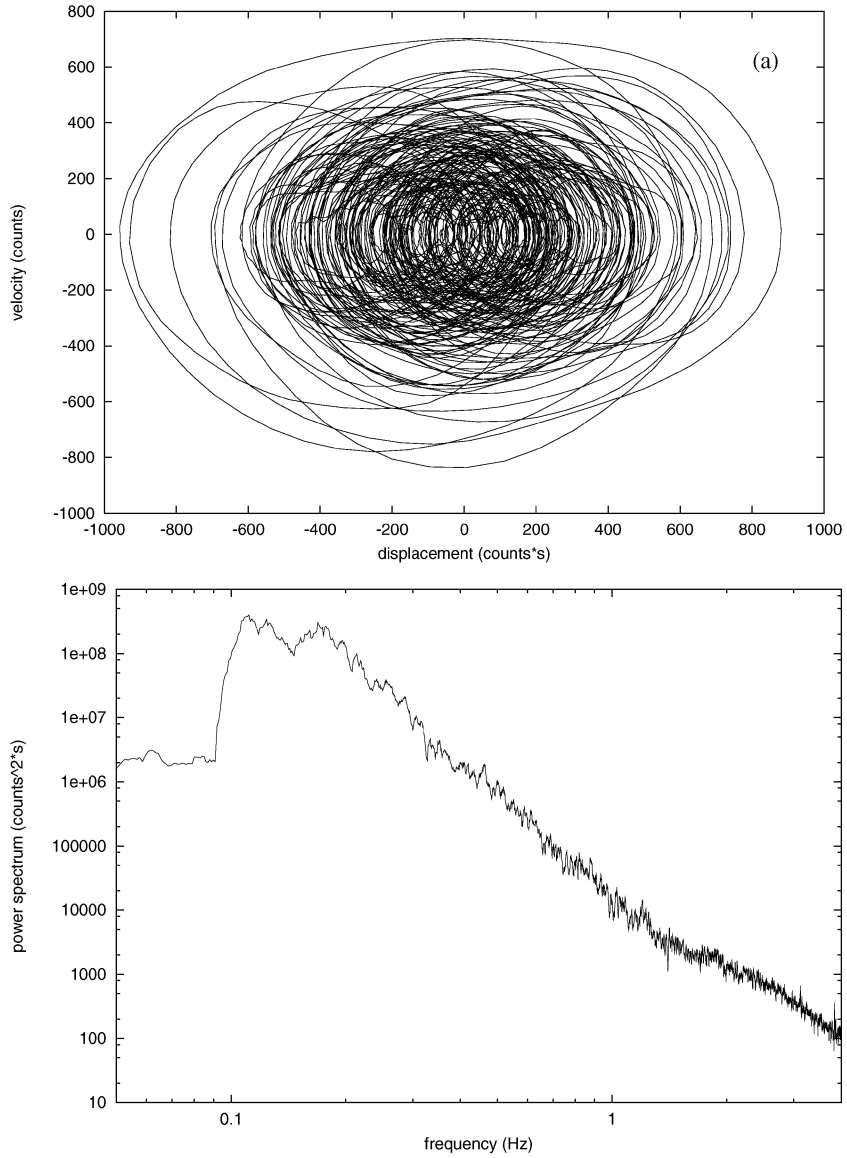


**Figure 3.** Power spectrum of the microseism time-series 950310.

$$\dot{q} = p$$
$$\dot{p} + \frac{\partial V_0(q)}{\partial q} + \delta p = \sum_{i=1}^{2} \gamma_i \cos(\omega_i t) + \varepsilon F(t) \tag{2}$$

where $V_0$ is the potential defined as

$$V_0 = -\alpha \frac{q^2}{2} + \beta \frac{q^4}{4} \tag{3}$$

and $\varepsilon$ is the amplitude of the random noise $F(t)$.

Observation (4) can be interpreted in terms of spatial and temporal variations of the source, that is, the cyclonic storm. Time pressure variations would imply slow variations of the central peak frequencies of the microseism. Variations in seabed topography along with variations in the thickness of the waveguide may account for the incoherent propagation of microseisms (Webb 1998). Stochasticity due to incoherent propagation can be modelled by randomizing the phase of the signal, that is, by randomizing the proper frequency $\alpha$ of the system (i.e. the response of a linear system in the absence of external forces), thus accounting for observation (7). The coefficient $\alpha$ that appears in eq. (3) in substitution of the coefficient $\alpha$ of eq. (1) is defined as

$$\alpha = \alpha_0 + \eta f(t). \tag{4}$$

where $\eta$ is the amplitude of $f(t)$, a white noise term. The coefficient $\alpha$ (or $\alpha_0$ if $\eta \neq 0$) can be positive or negative. For $\alpha < 0$ we are in the presence of only one potential well, whereas for $\alpha > 0$ there are two of them, known as the bistable potential.

On the other hand, spatial variations of the location of the storm would imply variations of the travel path. As microseisms are mainly composed of Rayleigh waves (guided waves), they should be very sensitive to the upper layered structure of the Earth. This would also account for observation (5), in which case we should also have to take into account seismic absorption, which would shift seismic waves to lower frequencies with increasing distances. The factor that takes into account the dissipation of energy is the damping coefficient $\delta$, and the amount of dissipation will depend on the length of the travel path. We then propose a phenomenological model, similar to the classical Longet-Higgins one but contemplated from a

different point of view. Instead of attempting to describe a travelling perturbation, our model eq. (2) describes the ground motion (the oscillatory motion generated by the non-linear oscillator) that would be recorded by a seismic station at a given distance from the source of microseismic activity. Looking at eq. (2) we can see that the model is composed of two contributions; medium properties on the left and external forces on the right.

## 4 PHASE SPACE AND POWER SPECTRUM

The broad-band records of microseism time-series that we have analysed consist of velocity records sampled at a rate of 80 Hz. The time-series has been integrated to obtain the displacement field, and the evolution of the system has been plotted in phase space (velocity vs displacement). Fig. 4 displays an example of the motion of a microseism time-series recorded on 95/03/10 at 03:00 for a time window of 1024 s, Fig. 4(a), and for a time window of 125 s, Fig. 4(b), to emphasize the details. As we can clearly observe, the motion follows well defined trajectories, similar to those of a particle bouncing irregularly in a potential well. This motion consists on a superposition of loops of different mean radius (i.e. motion with different frequencies) with the axis of the loops displaying separate irregular oscillations, over a well defined path. The corresponding motion is random in the sense that it is not possible to predict neither the time evolution of the axis of the loops nor the mean radius of the loop.

The evolution of microseism in phase space is qualitatively well represented by our model. Fig. 5 displays an example of the evolution in phase space of a time-series generated by eq. (2) with only one potential well, with the following numerical values of the parameters: $\delta = 0.01$, $\beta = 0.05$, $f_1 = 0.05$, $\gamma_1 = 7.5$, $f_2 = 0.2$, $\gamma_2 = 1.0$, $\varepsilon = 10.0$, $\alpha_0 = -4$, $\eta = 0.03$. The structure of motion in phase space is the same as in the case of microseisms: loops of different mean radius oscillating irregularly along a well defined path. Its power spectrum is presented in Fig. 6. It is composed of a main broad peak at 0.233 Hz, and another located at 0.198 Hz. The peak at 0.198 Hz corresponds to the external force $f_2$, whereas the peak at 0.330 Hz corresponds to the resonant frequency of the potential,

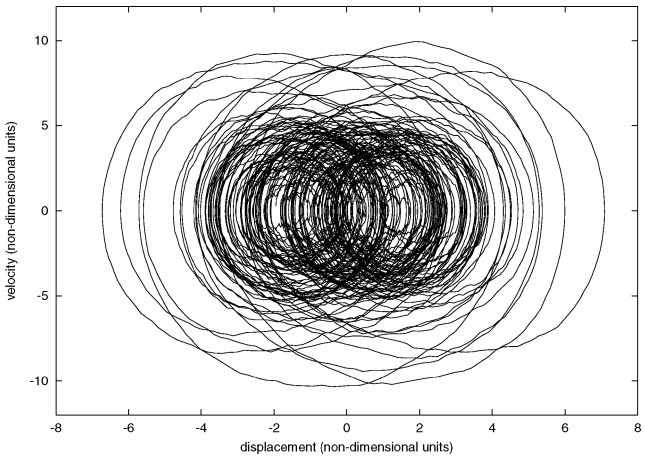


**Figure 5.** Motion in phase space of a time-series generated by the model eq. (2).

which has been obtained by generating a time-series with the same value of the parameters except that the force term is composed of only white noise.

In order to get some insight into the dynamical features of microseism time-series through our model, and to check its capacity to explain observations (4–7), a numerical study of the influence of the values of the parameters of eq. (2) has been performed. (As already stated, features (1–3) of microseism time-series, that is non-stationarity, stochasticity and non-linearity, are well reproduced by the model, as well as the shape of the power spectrum and the motion in phase space.) The parameters $f_1$ and $\gamma_1$ that characterize the low frequency external force and its amplitude, responsible for the motion of the axis of the loops, have been kept fixed in the numerical simulations, as they account only for the motion for long time scales.

### 4.1 Potential

The potential, eqs (3) and (4), is characterized by parameters $\alpha, \beta, \alpha_0$ and $\eta$. For $\beta = \eta = 0$ we are in the presence of the well known linear

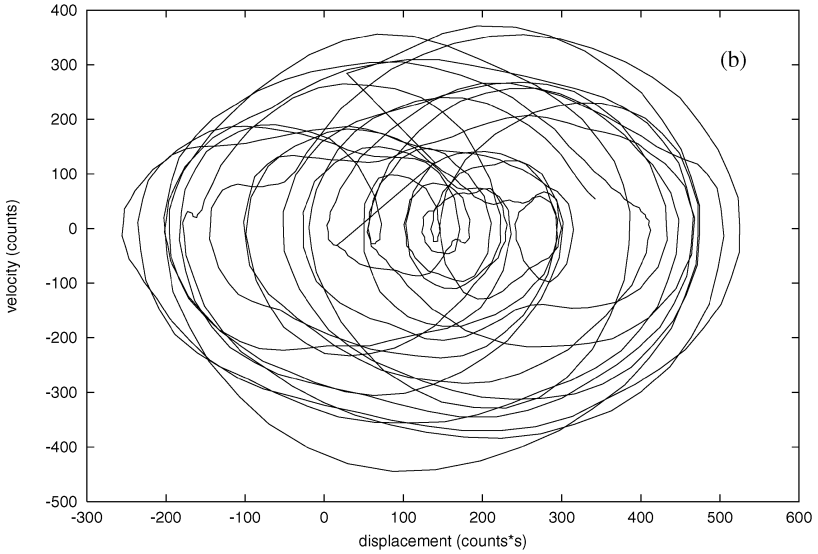


**Figure 4.** Motion in phase space of a microseism time-series recorded on 950310 at 03:00 for a time window of 1024 s (a) and of 125 s (b).

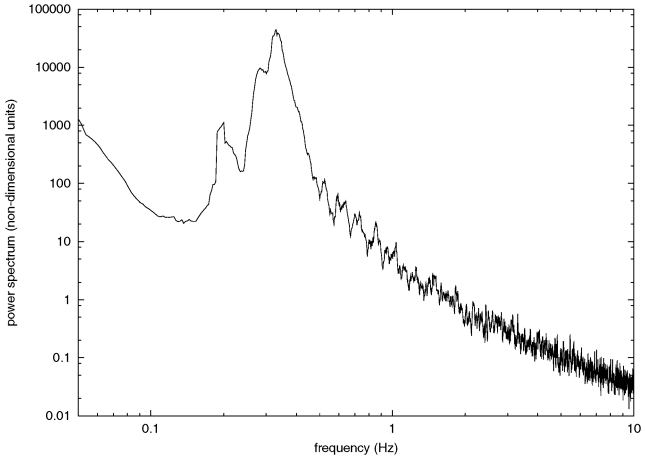


**Figure 6.** Power spectrum of the time-series presented in Fig. 5.

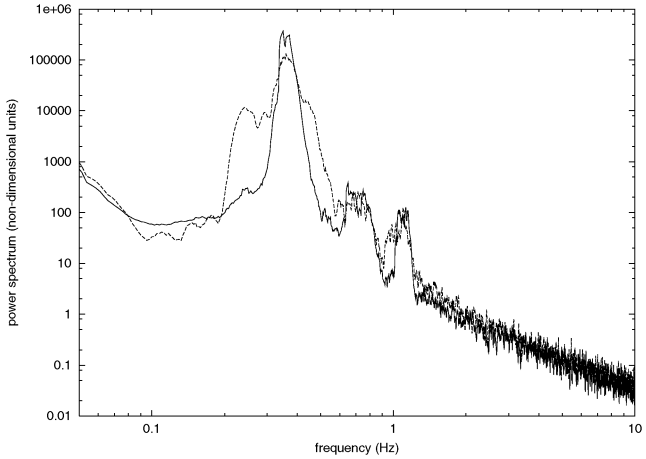


**Figure 8.** Evolution of the power spectrum as a function of the amplitude of the noise added to the resonance coefficient.

forced damped oscillator with noise. If $\beta \neq 0$ but $\eta = 0$ the system is non-linear and the frequency becomes dependent on the amplitude, so that the resonant frequency will be a slowly varying function. For the case $\beta = 0$, $\eta \neq 0$, the coefficient $\alpha$ will be time dependent $\alpha = \alpha(\alpha_0, t)$ and we will be in the presence of parametric resonance, i.e. a steadily increase of the amplitude of oscillations caused by the time variation of $\alpha$. In the more general case, with $\beta, \eta \neq 0$, the phenomenon of resonance will be the result of a competitive process between the time variation of $\alpha$ and the frequency of the external force, and contrary to the case of the linear oscillator, in the absence of damping the amplitude will grow without being singular.

First of all we have determined the resonant frequency for the following numerical values of the model parameters: $\alpha = -4.0$, $\eta = \gamma_1 = \gamma_2 = 0$, $\varepsilon = 1.0$, $\delta = 0.01$ and $\beta = 0.05$. The corresponding spectral peak (the resonant frequency) is located at $f_r = 0.34$ Hz. By introducing the parameters $f_1 = 0.05$, $\gamma_1 = 7.5$, $f_2 = 0.35$, $\gamma_2 = 1.0$ and $\eta = 0.03$, the shape and frequency of the resonant peak are preserved whereas new high frequency peaks have been generated. Fig. 7 displays the power spectrum of the oscillations for the above parameters, solid line; the shape is preserved for noise amplitudes up to $\varepsilon = 10.0$. For higher amplitudes of the additive noise, the amplitude of the spectral peak grows slightly and the peak broadens and is shifted to 0.4 Hz for a noise amplitude of $\varepsilon = 50$ (dashed line in Fig. 7). With respect to the higher harmonics, their central frequency also shifts to higher frequencies, although their amplitudes are reduced. It is of interest to observe an amplitude growth at both sides of the resonant peak, with only a slow variation in the amplitude of the resonant peak. Note also the generation of subharmonics in the power spectrum, one located at 0.171 for the continuous line and two located at 0.149 Hz and 0.205 Hz for the dashed line, and that the approximate relation 2 : 1 hold relative to the resonant peak.

With respect to the random variations of the resonant response, accounted for through the parameter $\eta$ defined in eq. (4), the influence of this additive noise on the resonant peak consists on a broadening of the peak, although preserving its central frequency for moderate values of $\eta$ and contributing, at the same time, to the generation of subharmonics, see Fig. 8 for $\eta = 0.00$ (continuous line) and $\eta = 0.06$ (dashed line).

The last term to be taken into account is the coefficient $\beta$ of non-linearity. Fig. 9 displays the variation of the spectral peak for $\beta = 0.00$ (continuous line), $\beta = 0.05$ (large dashed line) and $\beta = 0.10$ (short dashed line). A shifting to higher frequencies for increasing values of $\beta$ is clearly seen.

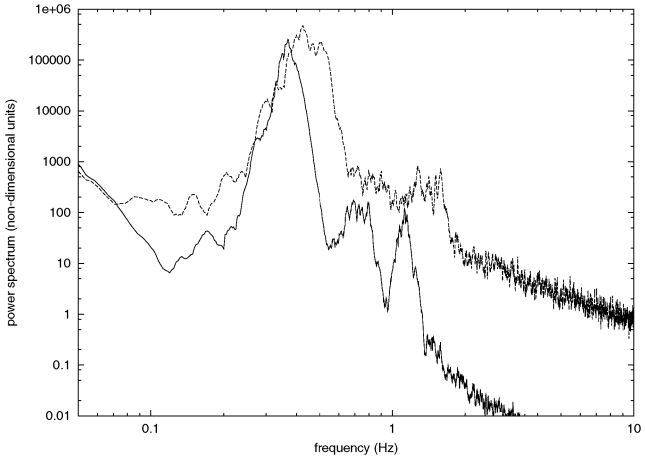


**Figure 7.** Evolution of the power spectrum as a function of the amplitude of additive noise.

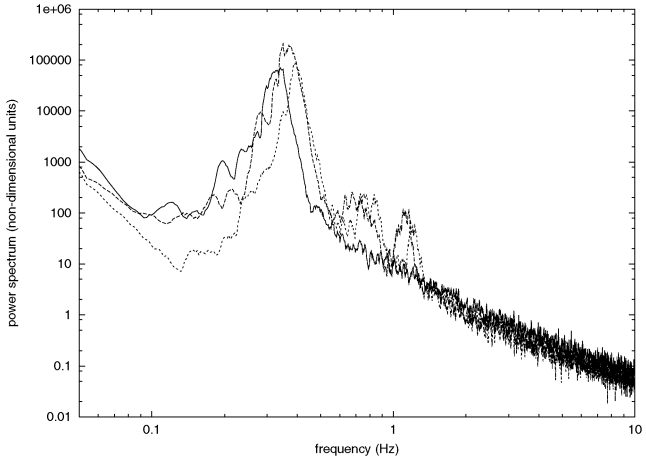


**Figure 9.** Evolution of the power spectrum as a function of the value of the coefficient of non-linearity.

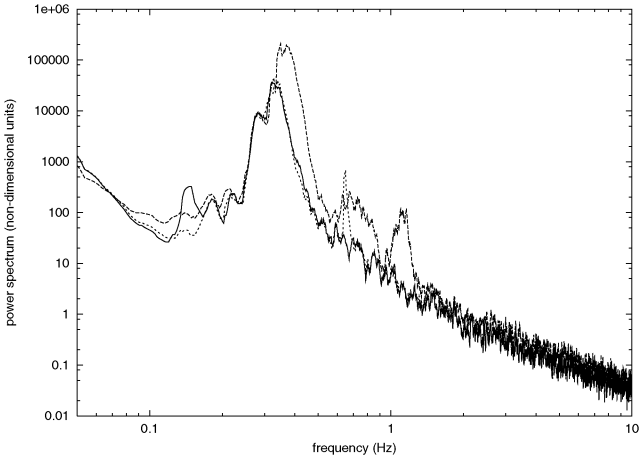


**Figure 10.** Evolution of the power spectrum as a function of the variation of the external frequency.

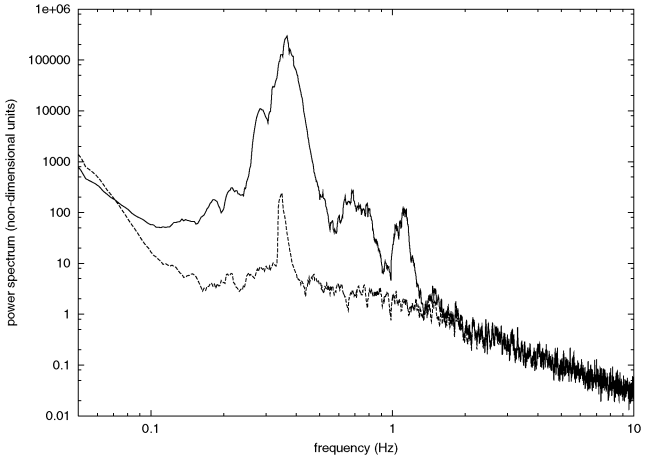


**Figure 12.** Evolution of the power spectrum as a function of the coefficient of damping.

### 4.2 External force and damping

The external force is characterized by two parameters: the frequency of the harmonic force and its amplitude. Fig. 10 shows the influence on the power spectrum of the variation of the frequency $f_2$ for a constant resonant frequency $f_r = 0.34$. For $f_2 = 0.15$ Hz (solid line) and $f_2 = 0.65$ Hz (short dashed line) their corresponding spectral peaks are present, the power spectra display only slight differences at low frequencies, and the shape and central frequency of the resonant peak are preserved. However, for an external frequency $f_2$ close to the resonant frequency (large dashed line), there appears to be an important growth and broadening of the resonant peak and of higher harmonics.

Fig. 11 shows the variation of the power spectrum due to variations of the amplitude of the external force for $\gamma_2 = 1.0$ (continuous line) and $\gamma_2 = 10.0$ (dashed line). There appears to be a slight transfer of energy from low to high frequencies and a magnification of the spectral peaks, specially at high frequencies. The influence of the amplitude of the additive noise has already been discussed in the preceding section.

Finally, Fig. 12 displays the variation of the power spectrum with the damping coefficient $\delta$. The effect is very pronounced for $\delta = 5.0$ (dashed line) with respect to $\delta = 0.0$ (solid line), for the frequency range 0.1 Hz–2.0 Hz. The amplitude reduction is quite severe, although the resonant peak is preserved. For low and high frequencies, both spectra coalesce.

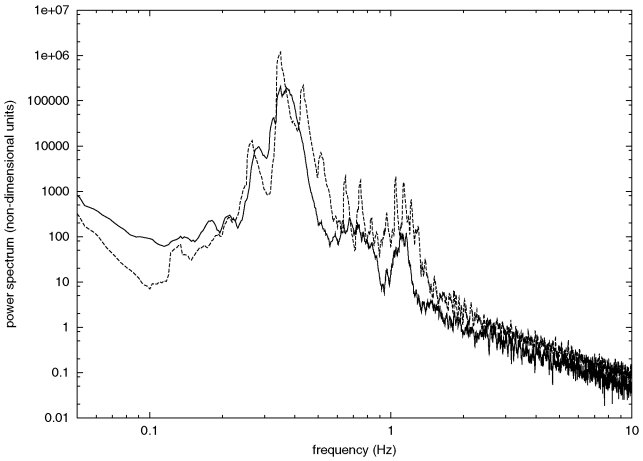


**Figure 11.** Evolution of the power spectrum as a function of the amplitude of the external force.

## 5 DISCUSSION AND CONCLUSIONS

Microseisms have been widely studied, both observationally and theoretically, through its power spectra, with the aim of improving the detectability of the arrival time of seismic waves. This problem is especially severe in planning seismic networks of Ocean Bottom Seismographs. As the main interest is focused on their power spectrum, linear theory suffices.

In the present study we have focused our interest on the time-series and its evolution in phase space, as well as in its power spectra. In a previous study CU found that these time-series are non-stationary stochastic and non linear, and that these characteristics were well reproduced by a non-linear forced, damped oscillator. In this study we have attempted to explain some commonly observed features (observations 4–7) by using a Duffing oscillator with additive noise as a predicting model. We do not claim that the model we have used is the model, but a phenomenological one, able to provide us with some insight on some properties of the time-series we have analysed. Moreover, as previously stated, we should emphasize that this study has the meaning of a 'mean field' one, in the sense that we are able to explain average properties (a study of the records of daily observations display severe fluctuations in power spectrum, see Fig. 3). Through numerical simulations with model eq. (2), the following results have been obtained.

A first result is that there is no need (although it does not means that the phenomenon does not exist) of a special source for the secondary spectral peak (at about half the frequency of the primary one). These primary peaks, or subharmonics, arise naturally because of the non-linearity of the system. The enhancement and broadening of the main peak can be explained in terms of a competitive process between the external force of frequency $f_2$ with additive driven noise, and the time varying parameter $\alpha$, giving rise to a parametric resonance. This competitive process, as opposed to superposition, is possible only in non-linear processes, and is thus governed by coefficient $\beta$. In this model, the random fluctuations of the coefficient $\alpha$ account for the observed incoherent propagation of microseisms, which in turn constitutes another source of non-linearity. Following Hasselmann (1963), the observed phenomenon of resonance can be interpreted in terms of the layered structure of the upper crust that acts as a waveguide. The variation of its thickness, along with

variations of medium properties (density and velocities) may act as a source of non-linearity.

Of fundamental importance is the damping coefficient $\delta$, which is able to explain the differences in the amplitude levels of the power spectra for stormy and quiet days (compare Figs 2 and 12), as well as its reduction to the same level at high frequencies. This behaviour cannot be obtained by amplitude variations of the external forces and/or amplitude of the additive noise, which effect mainly consist of broadening and shifting of the spectral peaks and of moderate amplitude variations. Thus, according to our model, the amplitude variations of microseisms should be due to the distance of the atmospheric storm instead of its strength: as there is a continuous transfer of energy from the atmosphere to the land surface and oceans and, due to solar heating, from land surface to the atmosphere, there will always be some atmospheric storm somewhere. Thereafter the term 'quiet day' has only a relative meaning. Quiet day is defined with respect to a given place, for which an atmospheric storm is far away. As an example, Hasselmann reports storms as a source of microseisms located at 11,500 km from the recording station. Similarly, a stormy day is that for which the source is relatively close (a few thousand km) to the recording location. Naturally, the intensity of the storm will undergo large fluctuations. The phenomenon of resonance can now be extended in the sense that the resonance is permanently excited through the combined action of atmospheric and oceanic activity that occurs at any location on the planet.

As generic features, we can say that a broadening of the spectral peak is achieved by increasing $\varepsilon$, $\eta$ and $\gamma_2$, whereas a shifting of the resonant peak to higher frequencies is obtained by increasing $\varepsilon$ and $\beta$. The secondary peaks or subharmonics naturally arise for $\varepsilon, \eta > 0$, whereas they vanish for increasing $\beta$. The amplitude variations are governed by $\delta$ and $\beta$. Table 1 summarizes the influence of the distinct parameters on the spectral shape of the microseism time-series.

The proposed model is able to explain the main average features observed for microseism time-series, i.e. the features listed in Section 2. Also, this model is minimalist in the sense that it contains the minimum number of parameters needed to explain observations, although not excluding other external contributions, such as coastal sea waves (Okeke & Asor 2000) or resonances generated by the geometry of coastal Fjords (Friedrich *et al.* 1998). As a novelty this model reveals that the main peak corresponds to the fundamental harmonic of the potential; that is, it represents a medium property, and when the frequency $f_2$ is close to the resonant frequency $f_r$, a competitive process is triggered which results in an enhancement of the resonant (secondary) peak.

The above interpretation is consistent with the discovery of the existence of free oscillations of the Earth in the absence of earthquakes for the frequency interval 0.001 Hz–0.01 Hz (Kanamori 1998; Nishida *et al.* 2000), resonances attributed to be generated by atmospheric turbulence. According to our model, the recorded ground motion in the absence of seismic activity can also be interpreted in terms of atmospheric turbulence of moderate wavelengths, that is, again a resonant process. The resonances for the interval 0.001 Hz–0.01 Hz would be related to the general atmospheric circulation. The interval 0.01 Hz–1 Hz would be related to the triple interaction cyclonic storm-ocean-Earth (Longuet-Higgins model). Finally, for frequencies higher than 1 Hz would be related to local meteorological activity along with cultural noise. The ubiquitous local meteorological activity, of random nature, justifies the additive noise term we have incorporated as a source term together with the external forces. From a global point of view, we can summarize the present study by saying that the observed resonant response of the earth, for the whole interval of frequencies, can be attributed to the coupling between the atmospheric turbulence and the Earth.

**Table 1.** Influence of the model parameters on the spectral features.

| Effects on | $\delta$ | $\alpha_0$ | $\eta$ | $\beta$ | $\gamma_2$ | $f_2$ | $\varepsilon$ |
|---|---|---|---|---|---|---|---|
| Resonant peak | | x | | | | | |
| Broadening | | | x | | | x | x |
| Amplitude | x | | | x | | | |
| Shifting | | | | x | | | x |
| Subharmonics | | | x | | x | x | x |

## ACKNOWLEDGMENTS

Peter Bormann read a first draft of the paper and his exhaustive comments are gratefully acknowledged. The comments of two anonymous referees greatly improved the manuscript; one of them drew Hasselmann's paper to my attention. Josep Vila provided the seismograms; he and Ramón Macià helped in the data analysis. This research was supported by the Dirección General para la Investigación Cientifica y Tecnológica under Grant PB96-0139-C04-02 and INTAS, Grant INTAS-952-139. M.U. was supported by a scholarship from the CIRIT under contract FI/95-1122. Contribution num 227 of the Dept. d'Astronomia i Meteorologia.

## REFERENCES

Abarbanel, H.D.I., Brown, R., Sidorowich, J.J. & Tsimring, L.S., 1993. The analysis of observed chaotic data in physical systems, *Rev. Mod. Phys.,* **65,** 1331–1392.

Aki, K. & Richards, P.G., 1980. *Quantitative Seismology,* Freeman, San Francisco.

Bath, M., 1973. *Introduction to Seismology,* Birkhauser Verlag, Basel.

Correig, A.M. & Urquizu, M., 1999. Dynamics of microseism time series (in Spanish), in, *100 anos de Observaciones Sismológicas en San Fernando,* pp. 203–213, eds Martin Davila, J. & Pazos, A. A., Boletin del Real Instituto y Observatorio de la Armada (ROA) 5/99, Ministerio de Defensa, Secretaria General Tecnica, San Fernando.

Friedrich, A., Krueger, F. & Klinge, K., 1998. Ocean-generated microseismic noise located with the Grafenberg array, *J. Seismol.,* **2,** 47–64.

Guckenheimer, J. & Holmes, P., 1997. *Non Nonlinear Oscillations, Dynamical Systems and Bifurcation of Vector Fields,*Springer-Verlag, New York.

Hasselmann, K., 1963. A statistical analysis of the generation of microseisms, *Rev. Geophys.,* **1,** 177–210.

Kanamori, H., 1998. Shaking without quaking, *Science,* **279,** 2063–2064.

Kantz, H. & Schreiber, T., 1997. *Nonlinear Time Series Analysis,* Cambridge University Press, Cambridge.

Kibblewhite, A.C. & Wu, C.Y., 1991. The theoretical description of wave-wave interactions as a noise source in the ocean, *J. acoust. Soc. Am.,* **89,** 2241–2252.

Lachet, C. & Bard, P.Y., 1994. Numerical and theoretical investigations on the possibilities and limitations of Nakamura's technique, *J. Phys. Earth,* **42,** 377–379.

Longuet-Higgins, M.S., 1950. A theory for the generation of microseisms, *Phil. Trans. R. Soc., Ser A,* **243,** 1–35.

Morikawa, H., Akamatsu, J., Nishimura, K., Onoue, K. & Kameda H., 1998. Stochastic simulation of microseisms using theory of conditional random fields, *Pure appl. Geophys.,* **151,** 81–99.

Nishida, K., Kobayashi, N. & Fukao, Y., 2000. Resonant oscillations between the solid earth and the atmosphere, *Science,* **287,** 2244–2246.

Okeke, E.O & Asor, V.E., 2000. On the microseisms associated with coastal sea waves, *Geophys. J. Int.,* **141,** 672–678.

Schreiber, T., 1998. Constrained randomization of time series data, *Phys. Rev. Lett.,* **80,** 2105–2108.

Theiler, J. & Prichard, D., 1996. Constrained realization Monte-Carlo method for hypothesis testing, *Physica D,* **94,** 221–235.

Vila, J., 1998. The broad band seismic station CAD (Tunel del Cadi, eastern

Pyrenees): site characteristics and background noise, *Bull. seism. Soc. Am.,* **88,** 297–303.

Webb, S.C., 1998. Broadband seismology and noise under the ocean, *Rev. Geophys.,* **36,** 105–142.

Wells, N., 1986. *The Atmosphere and Ocean; A Physical Introduction,* Taylor & Francis, London.

Wiecharet, E., 1904. Verhandlurgen der zweiten Internationalier Seismologischen Kouferenz, *Gerl. Beitr Geophys. Ergonzvngsband*, **2,** 41–43.

## APPENDIX

The following dynamical tests were applied by CU to analyse microseism time-series and time-series generated by a non-linear forced oscillator through eq. (2), with different values of the parameters and different levels of noise.

*Stationarity.* Many physical phenomena can be described in terms of statistical equilibrium, that is, if we consider a given interval of a time-series and divide it into subintervals, the distinct sections appear 'the same'. More precisely, we can say that the statistical properties of the process (the moments of different order) are independent of time. If this is the case, the process is stationary; and if not, non-stationary. The property of stationarity is crucial for subsequent calculations of dynamic invariants, like correlation dimension or redundancy. For the analysed data, time-series are clearly non-stationary.

*Autocorrelation.* The autocorrelation function of a linear process is a measure of the degree of dependence in the values of a time-series $s(t)$, delayed by an interval $\tau$ known as delay time. For a random process, the autocorrelation function fluctuates randomly around zero, indicating lack of memory of a given past time. For a periodic process, the autocorrelation function is also periodic, indicative of a close relation between values that repeat in time. The first zero crossing of the autocorrelation function is a measure of the time for which data are independent. This time is relevant in periodic systems because it may provide us with a criterion to select the delay time in phase space reconstruction. In the present case, the autocorrelation function displays a minimum at about 1 s.

*Coherence time.* The coherence time of the autocorrelation function is the time for which the absolute value of the autocorrelation is lower than a given $\varepsilon$ for all $t > \varepsilon$. If the autocorrelation function vanishes exponentially for $t \to \infty$, the coherence time is finite, and otherwise infinite. A long coherence time, of the order of the length of the analysed time-series, may be indicative of non-linearity. In our data we can distinguish two coherency times, a finite one of about 15 s, and a seemingly infinite one defined by an average value of the autocorrelation of 0.1 s. The influence of the infinite coherency time may be indicative of non-linearity.

*Mutual information.* Let $x$ and $y$ be two random variables (or, equivalently, two samples $s(t)$ and $s(t + \tau)$ of a time-series). The mutual information provides us with the amount of information that the variable $y$ contains on the variable $x$. The mutual information is computed in terms of Shanon entropy and can be viewed as a non-linear generalization of the autocorrelation function. If two samples are independent, the mutual information is zero. For a time-series, the first local minimum in the plot of mutual information vs delay time is considered a closer estimate of the optimal value of the time delay than the first zero crossing of the autocorrelation function (which is defined for linear processes). The mutual information presents a minimum at 1 s, as for the case of autocorrelation.

*Redundancy.* Constitutes an extension of mutual information, which is defined for two dimensions (variables), to $n$-dimensions (variables). One should distinguish between redundancy and linear redundancy. Linear redundancy is computed from the correlation matrix of a given time-series and constitutes a characterization of its linear structure. Thus, if by comparing linear redundancy and redundancy we observe significantly different structures, we can assert the presence of non-linearity. For the embedding dimensions $m = 2, \ldots, 10$, the structure of the curves of the linear redundancy and the redundancy are significantly different, thus providing strong evidence in favour of non-linearity in the system.

*Correlation dimension.* The dynamics of a dissipative deterministic system is defined by the geometry of the attractor in the phase space (the region where a dissipative system evolves once the transients have vanished). If the attractor is of low dimension the system is deterministic; otherwise it is, or behaves as, stochastic. A good approximation of the attractor's dimension is provided by the correlation dimension, computed from the correlation integral. The correlation integral is defined as the fraction of all pairs of points on the attractor with distance less than a given distance $\varepsilon$, and is computed for a range of distances. The power law dependence of the correlation integral on $\varepsilon$ enables its exponent to be calculated when the distance tends to zero. The correlation dimension of the attractor is the limiting value of the exponent in phase spaces of increasing dimension. For the analysed data, the correlation dimension saturates to a value close to 5 for a delay time $\tau$ of about 0.25 s, but do not saturate for $\tau \sim 1$ as suggested by the mutual information. We thus conclude that microseisms behave stochastically.

*Surrogate data.* Surrogate data consist of a series of artificially generated data for use instead of the original time-series, and provide a baseline for comparison with the original data. In other words, this method gives us a mechanism to test null hypothesis. Surrogate data are generated from random process in such a way that the autocorrelation function of the original time-series is preserved. A widely used way to generate surrogate data is to apply the Fourier transform to the original time-series, randomizing the phases and applying the inverse Fourier transform. If, when analysing a set of surrogate data, we get the same result as for the original time-series (for example a low-dimensional chaotic system), the null hypothesis cannot be rejected (i.e. the series is not chaotic). In the present analysis the series of surrogate data present the same characteristics as the original time-series, as far as correlation dimension analysis is concerned, and their phase spectra display random behaviour, similar to a random walk. Hence, we must rule out any deterministic character of observations.

*Determinism versus stochasticity (DVS).* This test consists in fitting a set of locally linear models to several sets of data. Once the different models are fitted, the precision of each short-term prediction for an interval of data not used in the fit is computed. If the error is lower for a short interval of data points than for a longer one, it is inferred that the time-series is deterministic and non-linear. If, on the contrary, the minimum is for a longer interval (longer prediction time), the underlying system is stochastic. This test has been applied for embedding dimensions $m = 2, 4, 6, 8$ and for a time delay on one sample (results are independent of the time delay used). For all dimensions the prediction error is higher for the larger number of points used for the local prediction, up to a constant value. This behaviour is indicative of the stochasticity of the time-series.

As a consequence, we conclude that microseism time-series are *non-stationary, stochastic and non-linear*.